Surface Review and Letters, Vol. 9, No. 2 (2002) 1243–1250

THE FERMI SURFACE IN A MAGNETIC METAL–INSULATOR INTERFACE

T. GREBER, W. AUWÄRTER, M. HOESCH, G. GRAD,*
P. BLAHA* and J. OSTERWALDER
Physik-Institut, Universität Zürich, Winterthurerstrasse 190, CH-8057 Zürich, Switzerland
**Institute of Physical and Theoretical Chemistry, TU Vienna, Getreidemarkt 9/156, A-1060 Vienna, Austria*

Nickel (111) and the interface of hexagonal boron nitride on Ni(111) serve as model systems for an itinerant ferromagnet that is truncated with vacuum or a single layer insulator. These systems are investigated with angle-scanned He I and He II photoemission. Upon formation of the *h*-BN/Ni(111) interface the work function drops by 1.8 eV and the minority Ni Λ_3 *d*-band shifts by 0.13 eV to higher binding energy. This indicates that the Ni magnetic moment decreases in the interface. Spin-polarized band structure calculations from bulk nickel identify the observed minority and majority bands. The experimental Fermi surface maps show that *h*-BN distorts a minority *d*-band in a way which is consistent with the decreasing magnetic moment. It can be seen that *h*-BN affects the scattering of the electrons. Effects in the photoemission final and initial state are recognized.

1. Introduction

The electronic structure in interfaces is of key importance for the understanding and tailoring of electron junctions. In metallic systems the Fermi surface conditions electron transport. The disruption of the bulk periodicity at surfaces or interfaces modifies the classical picture of the Fermi surface: The electrons scatter at a surface which gives rise to standing wave patterns, i.e. spatial modulations in the electron density, known as Friedel oscillations, and to localized surface or interface states. Furthermore, electron tunneling may occur and the corresponding transmission depends on the **k**-vectors of the electrons. All these properties rely on the potential across the interface. The potential is affected by the charge transfer upon bonding between the materials that constitute the interface and in a self-consistent way by the Friedel oscillations. In magnetic systems the interface junction is different for electrons with parallel and antiparallel spins, respectively. This is for example reflected in the variation of the magnetic moments in an interface[1] and gives rise to phenomena like the giant magnetoresistance(GMR)[2] and/or spin selective tunneling.[3]

Photoemission is the method of choice for the task of measuring the dispersion of occupied states throughout the Brillouin zone. Of course, at an interface the concept of the bulk Brillouin zone does not hold. The periodicity breaks down and it is a formidable and yet unsolved task to resolve the electronic states in momentum *and* space. It is for example not clear to which extent the observed band structure corresponds to the average band structure within the probing depth Λ.

In order to study such effects, atomically sharp and well-defined interfaces have to be at hand. For this purpose we use the model system of single layer hexagonal boron nitride on Ni(111).[4] Results from photoemission experiments with He Iα and He IIα radiation are presented. Cuts across the Fermi surfaces of the bare Ni(111) and a monoatomic layer of hexagonal boron nitride on Ni(111) are compared. The experiments are discussed in connection with density functional calculations.[5] It is shown that

the nonmagnetic insulator acts as a two-dimensional grating that modifies the Ni bulk Fermi surface near the interface.[6]

2. Experimental

The experiments were performed in a modified Vg ESCALAB 220 photoelectron spectrometer with He Iα ($\hbar\omega$ = 21.2 eV) and He IIα ($\hbar\omega$ = 40.8 eV) radiation.[7] These two photon energies are used to probe two two-dimensional sections in k-space. The overall energy/momentum resolution was better than 50 meV/0.02 Å^{-1} FWHM and all presented data were taken at room temperature. $k_\parallel$ is determined from the electron kinetic energy in the vacuum ($E_{\rm kin}^{\rm vac} \equiv \hbar\omega - \Phi - E_B$) and the polar emission angle θ with respect to the surface normal: $k_\parallel = \sin(\theta)\sqrt{2m_e E_{\rm kin}^{\rm vac}}/\hbar$. E_B is the electron binding energy relative to the Fermi level. The work function was determined from spectra taken at normal emission with a bias voltage of -9 V applied to the sample in order to resolve the secondary electron emission cutoff. From the width ΔE of the spectra the work function $\Phi = \hbar\omega - \Delta E$ is determined. For Ni(111) a work function of 5.3 eV and for h-BN/Ni(111) of 3.5 eV is found in agreement with Nagashima *et al.*[4,8]

The sample preparation and characterization is described elsewhere.[4,9] h-BN forms perfect (1×1) commensurate monolayers on Ni(111) and its structure is well known.[9–11]

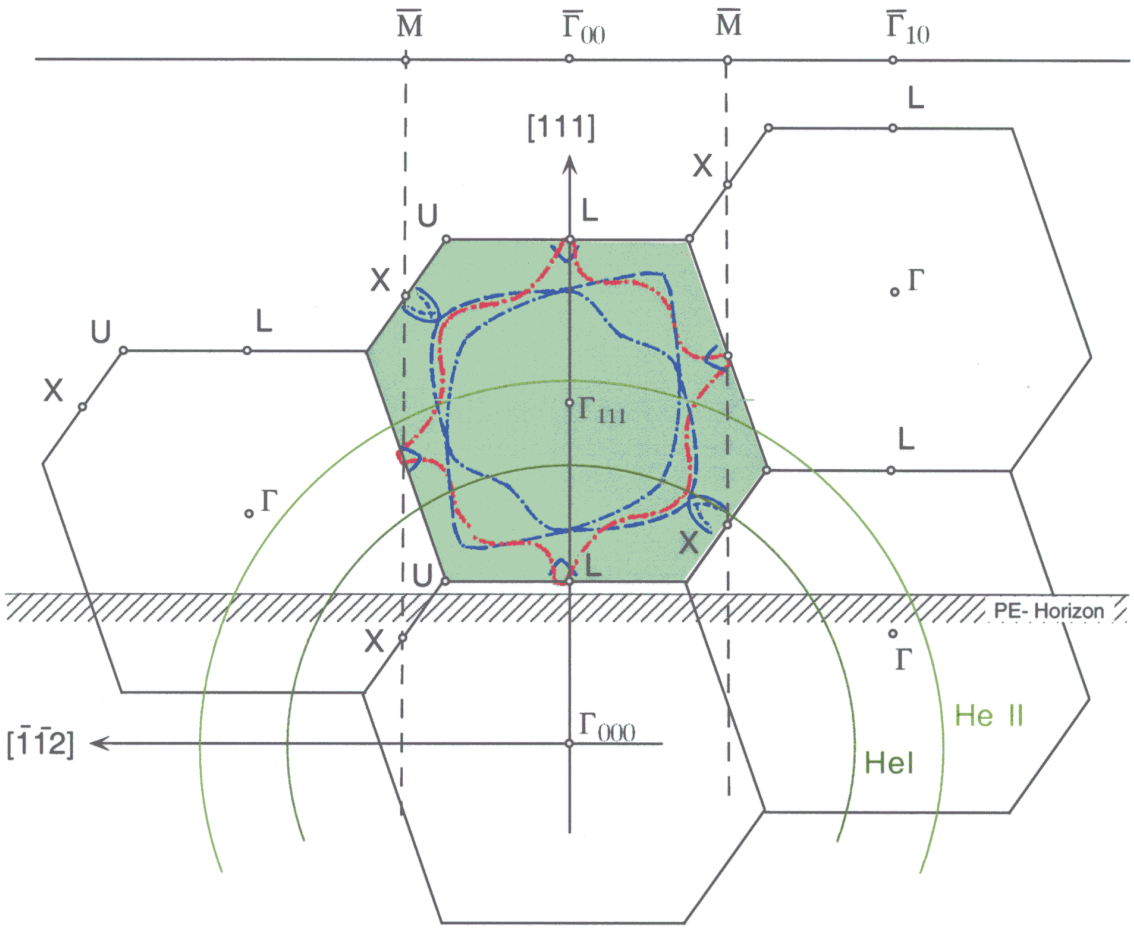

Fig. 1. Schematic diagram for k-space mapping experiments. In the free final state approximation direct transitions are expected if the free final state sphere intersects with an initial state band in the extended zone scheme. $\mathbf{k}_\parallel$ of this intersection point is conserved throughout the whole photoemission process and can be determined in an angle-resolved experiment. The photoemission (PE) horizon is imposed by the inner potential that has to be overcome in order to promote electrons into the vacuum.

3. k-Space Mapping

In Fig. 1 an angle-scanned photoemission experiment is illustrated in a $k_\perp$ vs. $k_\parallel$ picture as it was put forward by Aebi *et al.*[12,13] The k-space of an fcc crystal with a (111) surface is chosen, where $k_\parallel$ points along the $[11\bar{2}]$ direction. The initial state bands are displayed for a given energy (e.g. the Fermi energy) in a periodic zone scheme. The free final state band is a sphere centered at Γ_{000} and has an energy $\hbar\omega$ higher than the initial states. It corresponds to a spherical surface centered at Γ_{000} with a radius of $\mathrm{k}_f = \sqrt{2m_e(E_{\mathrm{kin}}^{\mathrm{vac}} + U)}/\hbar$. U is the inner potential which is set to 10.7 eV for Ni(111).[14] At any intersection point between an initial state band and the final state band, a resonance occurs. This translates such a k-point into a direction with enhanced emission intensity. The momentum of the photon is neglected and direct transitions obey the momentum conservation

$$\mathbf{k}_f = \mathbf{k}_i + \mathbf{G}\,, \qquad (1)$$

where $\mathbf{k}_f$ is the final state wave vector inside the solid, $\mathbf{k}_i$ the initial state wave vector and $\mathbf{G}$ a reciprocal lattice vector of the three-dimensional bulk lattice *and/or* two-dimensional surface lattice. It is most convenient to display the photoemission intensities inparallel projection, i.e. as a function of $\mathbf{k}_\parallel$.

For the case of ferromagnetic nickel, minority and majority bands have to be considered. In order to measure the spin polarization the sample has to be magnetized macroscopically and spin polarimeters have to be used. On samples which were not macroscopically magnetized, band structure calculations may identify the spin of the individual transitions. In Fig. 1 the band calculations of Tsui are shown.[15] The free final state spheres for He I and He II are indicated as well. It can be seen that photoemission at these energies mainly samples the Brillouin zone which contains Γ_{111} since no photoelectrons can be measured below the photoemission horizon that is imposed by the inner potential.

4. Results and Discussion

In Fig. 2 He I excited photoemission spectra for Ni(111) and h-BN/Ni(111) are shown for normal emission. The most prominent features upon formation of the h-BN layer are the BN related σ and π bands at 5.3 and 10.0 eV binding energy. It is seen that the Ni d-band related emission features get attenuated by a factor of ≈ 3, which indicates a short mean free path for these electrons. The work function shifts by 1.8 eV, from 5.3 eV to 3.5 eV. This work function decrease signals that the h-BN layer acts as an electron donor to the nickel substrate. Self-consistent field (scf) calculations for a single (free-standing) layer of h-BN with the experimental corrugation[9] but without substrate, indicate a charge transfer of 0.56 e^- from boron to nitrogen. This charge transfer is due to the higher electronegativity of nitrogen and makes h-BN an insulator. The numerical value was determined from the charge difference between a superposition of neutral atomic densities and the fully converged scf results. The charge on the atoms was determined according to Bader[16] by integration over an atomic basin.[17] In the case of h-BN/Ni(111) the Bader procedure yields a charge of 0.59 electrons on nitrogen and $-0.65e^-$ on boron. Therefore the net charge transfer to the substrate is 0.06 electrons per unit cell and the ionicity of the BN bonds even increases. Within an electrostatic picture where a charge separation length of 1 Å is assumed, this yields a work function shift of 2 eV, which gives the correct sign and order of magnitude. In a rigid band shift picture this charge is mainly transfered into the Ni d-band since its density of states is much larger than that of the sp-bands. From this we expect a decrease of the magnetic moment in the interface since there are empty minority d-states available only. Slab calculations do indeed support

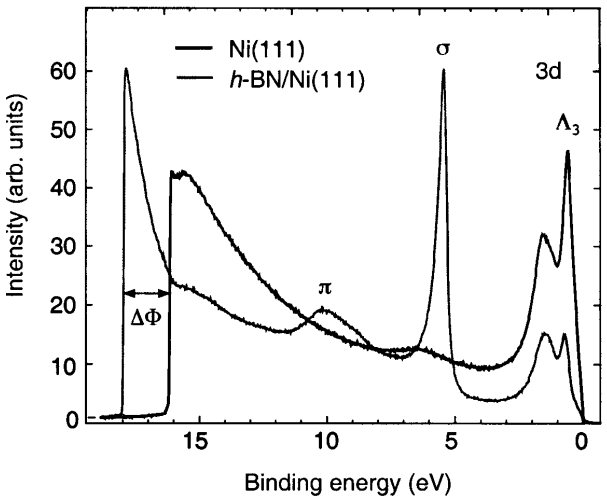

Fig. 2. He I normal emission UP spectra for Ni(111) and h-BN/Ni(111). The work function decrease upon formation of the h-BN layer indicates a decrease of the Ni magnetic moment (for details see text).

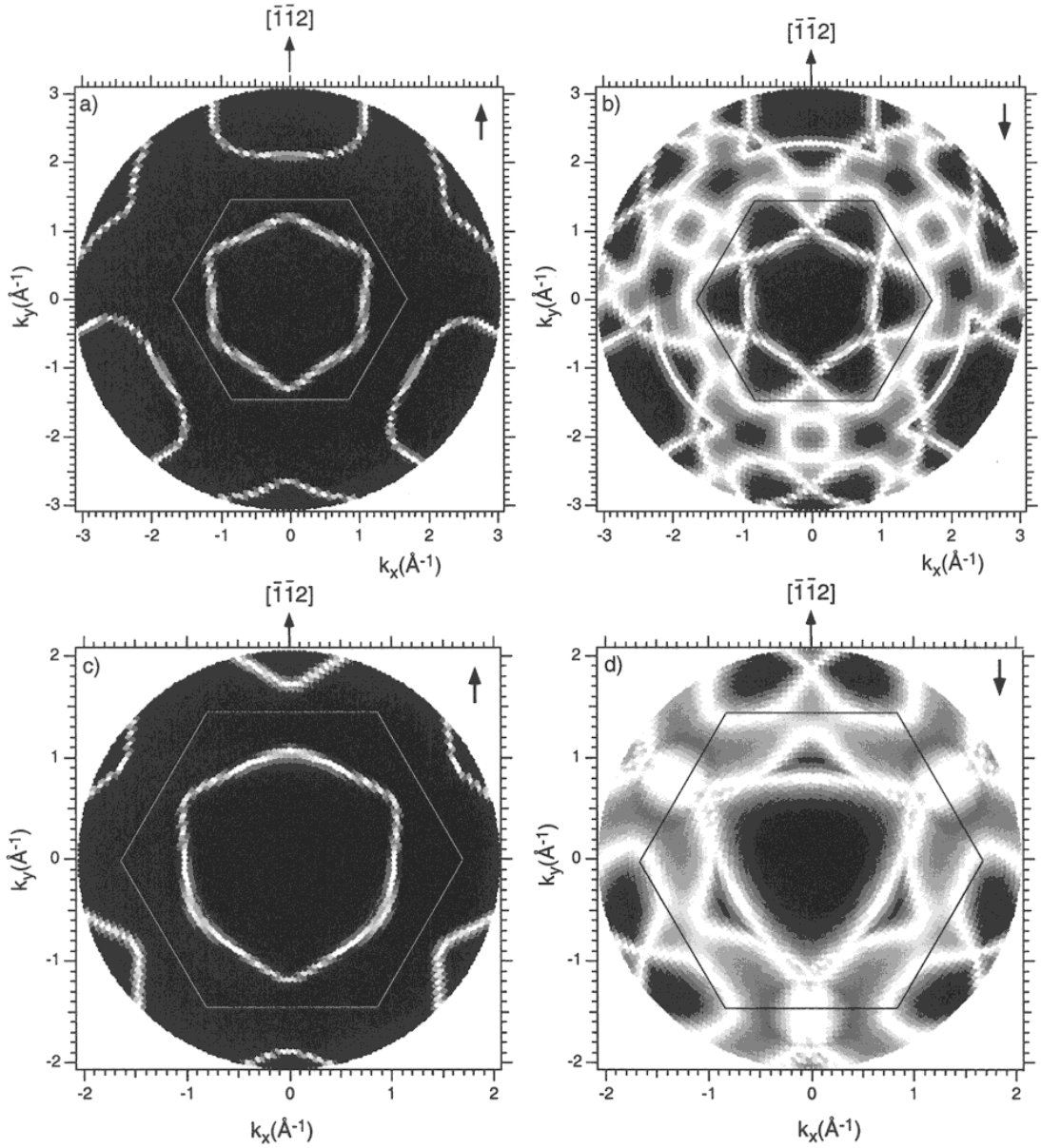

Fig. 3. Fermi surface maps as they were expected from the free final state approximation and calculated nickel bulk bands ($U = 10.7$ eV, $\Phi = 5.3$ eV). Direct transitions shine up as bright bands. (a) He II excited majority (up) bands; (b) He II excited minority (down) bands; (c) He I excited majority (up) bands; (d) He I excited minority (down) bands. Clearly the maps in (a) and (c) indicate *sp*-bands only, while the minority maps in (b) and (d) show in addition rich *d*-band structures.

this picture.[18] This is further backed by the observed Λ_3 minority *d*-band shift from 0.54 to 0.67 eV binding energy, which is consistent with the decrease of the Ni magnetic moment near the interface.

Before we study the influence of the *h*-BN on the Fermi surface, we display calculated Fermi surface maps for the two photon energies. In Fig. 3 such k-space maps for bulk Ni are shown. They were determined from spin-resolved band structure calculations as performed with the Wien code[5] for He I and He II free electron final states (see Fig. 1). They are parallel-projected cuts of spheres in the periodic zone scheme. The patterns have threefold rotational symmetry (C_{3v}) as it is expected from fcc symmetry

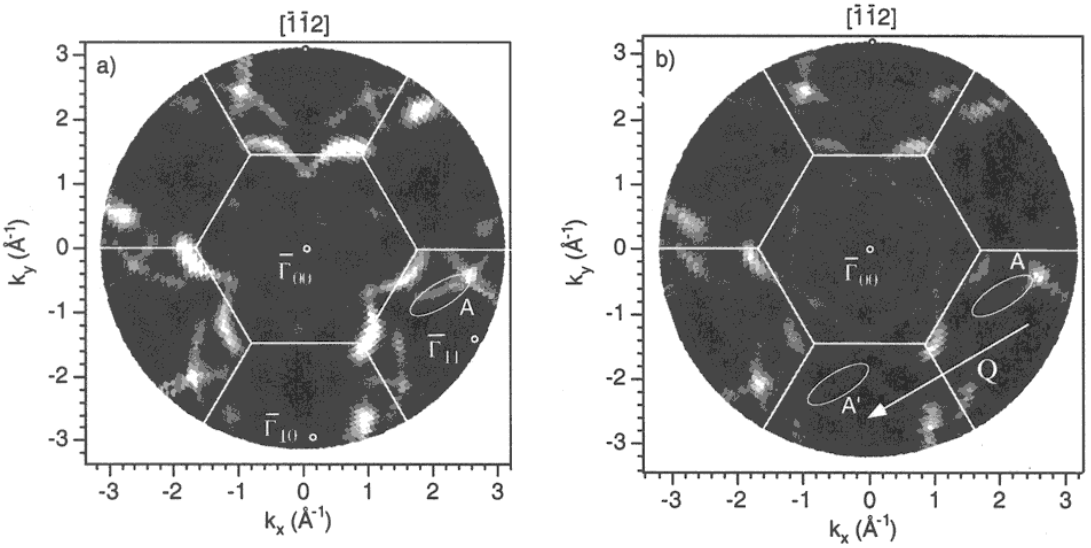

Fig. 4. He II Fermi surface maps as measured by angle-resolved photoemission. The intensity on a linear gray scale (white means high intensity) is displayed as a function of $\sin(\theta)$ and φ, θ being the polar and φ the azimuthal emission angle. The high-symmetry direction $[\bar{1}\bar{1}2]$ is indicated. (a) Ni(111) ($k_\parallel \leq 3.05$ Å^{-1}); (b) h-BN/Ni(111) ($k_\parallel \leq 3.13$ Å^{-1}). The feature A is shifted upon the formation of the h-BN interface and appears umklapped (A') by a surface reciprocal lattice vector $\mathbf{Q}$.

along [111]. The picture for majority spins is particularly simple since in Ni the majority d-band is full and states of the sp-band only emerge at the Fermi energy. In the case of the minority spins the Fermi surface is much richer due to the presence of the open d-bands.

In Fig. 4 He II excited Fermi surface maps are shown for Ni(111) and h-BN/Ni(111). The photoemission intensity from the Fermi level is displayed on a linear gray scale for different emission angles in parallel projection. The maps correspond to a two-dimensional cut across the k-space (see Fig. 1). The "star"-like feature centered in the first surface Brillouin zone has almost perfect sixfold symmetry. Two different second surface Brillouin zones are identified, i.e. the Fermi surface cut returns to threefold symmetry. The sixfold symmetry in the first surface Brillouin zone is due to the fact that the final state sphere cuts k-space close to Γ_{111}, i.e. $k_\perp + G_\perp = 0$, where $G_\perp = \sqrt{6}\pi/a$ is a reciprocal lattice vector along [111] and $a = 2.49$ Å is the surface lattice constant (see Fig. 1). The influence of the h-BN is weak. A careful comparison of the Fermi surface maps in Fig. 4(a) and 4(b), however, indicates a faint additional band A' in the second surface Brillouin zone which contains $\bar{\Gamma}_{10}$. It can be rationalized by umklapps of feature A in the Brillouin zone with $\bar{\Gamma}_{11}$. The length of the umklapp vector $\mathbf{Q}$ is $|\mathbf{Q}| = \frac{2\pi}{a}\frac{2}{\sqrt{3}} = 2.9$ Å^{-1}. From comparison with Fig. 3 it is seen that the umklapps of type $A \rightarrow A'$ in Fig. 4 are d-band-related. It is an indication for the influence of the interface on the electronic structure. From shifts in energy or momentum of particular transitions we get more quantitative information on the effect of the interface on the electronic structure.

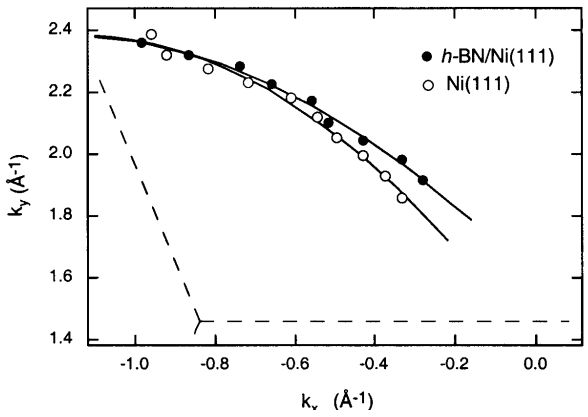

Fig. 5. Fermi surface distortion upon the formation of the h-BN interface. The A-type d-band feature shifts and indicates a decrease in minority d-holes. The dashed lines are surface Brillouin zone boundaries.

Figure 5 illustrates the distortion of the Fermi surface. The *d*-band features of type *A* in Fig. 4 are extracted by fitting local maxima in the Fermi surface contours for Ni(111) and *h*-BN/Ni(111), respectively. Clearly the *d*-band gets shifted up to 0.1 Å^{-1}, which corresponds to a few per cent of the diameter of the Brillouin zone. The trend can again be understood with the filling of the minority *d*-band upon charge transfer from the *h*-BN layer since it is equivalent to a decrease of the minority *d*-hole pocket.

In Fig. 6 He I excited Fermi surface maps of bare Ni(111) and *h*-BN/Ni(111) are shown. The influence of the *h*-BN is more pronounced than in the He II Fermi surface cut (see Fig. 4). The He I Fermi surface map of Ni(111) has threefold rotational symmetry C_{3v} [Fig. 6(a)] and fits the calculated pattern [see Figs. 3(c) and 3(d)] remarkably well. The Fermi surface map of *h*-BN/Ni(111) is as well threefold-symmetric since the structure of the *h*-BN overlayer has C_{3v} symmetry too.[9,10] However, in comparing Fig. 6(a) and 6(b) it can be seen that *h*-BN strongly influences the observed Fermi surface cut. This is surprising since an insulator should contribute no new states at the Fermi level. In Fig. 6 we consider the two features *B* and *C*, which contain majority *sp*-bands and minority *d*- and *sp*-bands.[19] It is seen that with *h*-BN these features are replicated into B' and C'. It is intriguing to make a correspondence between the originals as inferred from the bare Ni(111) and the replicas. From their shape a correspondence $B \rightarrow B'$ and $C \rightarrow C'$ is likely. They are shifted by a vector $\mathbf{Q}_{\text{exp}}(B \rightarrow B')$ and $\mathbf{Q}_{\text{exp}}(C \rightarrow C')$ of 3.1 ± 0.1 Å^{-1}, parallel to the primitive reciprocal surface lattice vector $\mathbf{Q}$ with $|\mathbf{Q}| = 2.9$ Å^{-1}. The $B \rightarrow C'$ and the $C \rightarrow B'$ correspondence is another possible assignment. This assignment has to be favored above the umklapps if the peak positions are considered and if they correspond to a rotation of *B* and *C* by π (or $\pm\pi/3$). This can be explained by reflection of the initial states at the boron nitride (see below). It has the consequence that near the interface the bulk Brillouin zone gets smaller, i.e. backfolded and hexagonal.

In the following the observed photoelectron scattering which is caused by the *h*-BN overlayer will be discussed. From electron diffraction experiments at low energies (V-LEED) it is known that the electron reflection is strongly energy-dependent[21] and for example even sensitive to adsorbed hydrogen.[22] Therefore, it is difficult to interpret changes in photoemission intensities without a complete model which takes the final state scattering into account.[6]

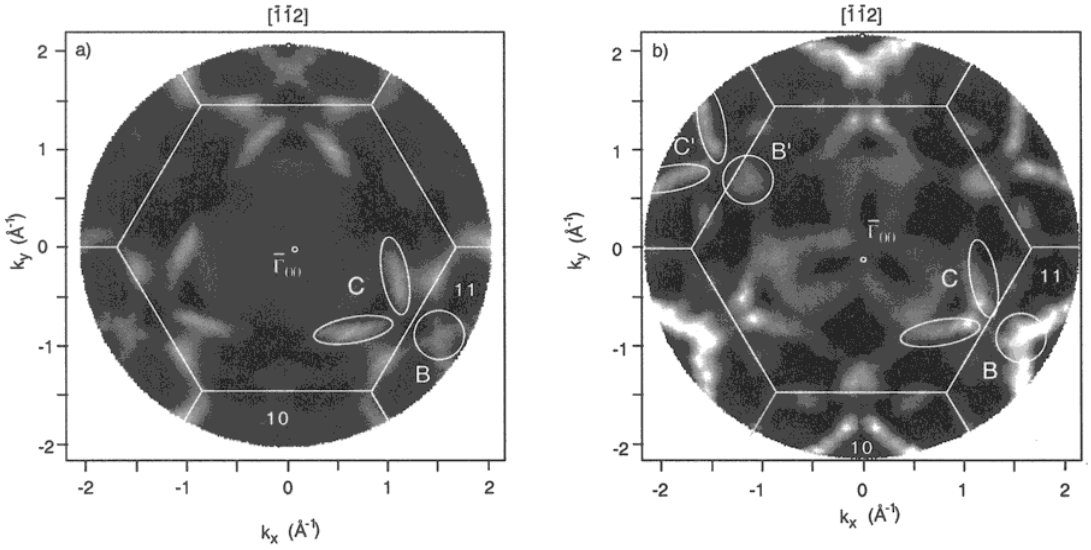

Fig. 6. He Iα Fermi surface maps. (a) Ni(111) ($k_{\parallel} \leq 2.04$ Å^{-1}); (b) *h*-BN/Ni(111) ($k_{\parallel} \leq 2.15$ Å^{-1}). The features *B* and *C* are replicated three more times. The assignments $B \rightarrow B'$ and $C \rightarrow C'$ indicate surface umklapps while $B \rightarrow C'$ and $C \rightarrow B'$ signal standing waves due to reflection of the initial states on the interface plane.

Table 1. Elastic scattering cross sections as determined from the scattering of an electron plane wave on B and N for the relevant energies E_F, E_F + He I and E_F + He II.

Energy (eV)	$\sigma_{\rm el}(B)$ (Å^2)	$\sigma_{\rm el}(N)$ (Å^2)
7.1	12.8	13.7
28.3	5.3	4.9
47.9	3.4	3.5

In Table 1 the elastic scattering cross sections for boron and nitrogen are summarized for three different energies.[20] The elastic scattering cross sections $\sigma_{\rm el}$ follow the $1/k$ trend. $\sigma_{\rm el}$ is fairly large if it is compared to the size of the 1×1 surface unit cell of Ni(111) (5.4 Å^2). A photoelectron that penetrates into this h-BN layer may therefore be strongly scattered. The simple plane wave scattering calculation gives the order of magnitude of the effect only, since the influence of interference between B and N and multiple scattering is not considered. The larger $\sigma_{\rm el}$ for He I compared to He II final states is in line with the weaker "replicas" in the He II Fermi surface map. The question how the ground state wave function is affected by the h-BN overlayer is most important. In photoemission it is *a priori* not possible to decide whether replicas as reported above are intrinsic ground state properties and/or a pure effect of elastic final state scattering. From Table 1 it follows that the scattering cross section is larger for initial state electrons at the Fermi energy than for those in the final state. In any case, the interface acts as a grating for all kinds of electrons. Grating means a periodic object on which the electrons are scattered in a coherent way. This scattering may be reflection, transmission and/or diffraction. Below the diffraction limit, zero order diffraction, i.e. reflection (and eventually transmission), persists. For reflection of a state $\Psi(\mathbf{k}_i)$ on the interface this means that for $\mathbf{k}_i = \mathbf{k}_{i\parallel} + \mathbf{k}_{i\perp}$ a state at $\mathbf{k'}_i = \mathbf{k}_{i\parallel} - \mathbf{k}_{i\perp}$ should exist. This state $\Psi(\mathbf{k'}_i)$ cannot be unambiguously distinguished from $\Psi(\mathbf{k}_i)$ by photoemission since $\Psi(\mathbf{k}_i)$ and $\Psi(\mathbf{k'}_i)$ have the same $\mathbf{k}_{i\parallel}$ value. However, from time inversion symmetry a state at $\mathbf{k''}_i = -\mathbf{k'}_i$ exists as well and this state at $\mathbf{k''}_i = -\mathbf{k}_{i\parallel} + \mathbf{k}_{i\perp}$ can be observed by photoemission. Of course, reflection may be observed only in the initial state since reflection of the final state does not allow the detection. In the present case of an fcc (111) surface reflection is equivalent to a rotation of the corresponding Fermi surface pattern by π or $\pm\pi/3$, respectively(see Fig. 1). Therefore standing wave patterns $|\Psi(\mathbf{k}_i) + \Psi(\mathbf{k'}_i)|^2$ can be evidenced by the observation of states at $\mathbf{k''}_i$ which were replicas of states at $\mathbf{k}_i$. It will be interesting (and necessary) to explore the phase shift between the incoming (unscattered) wave $\Psi(\mathbf{k}_i)$ and the reflected (scattered) wave $\Psi(\mathbf{k'}_i)$. This phase shift will influence the spatial photoemission cross section, i.e. the layer from which a particular state is excited, and is of importance for the answer to the question why these signals for standing waves are not seen on the bare nickel.

5. Conclusions

The work function drop upon formation of a h-BN layer on Ni(111) and the decrease in binding energy of the Λ_3 band indicate a lowering of Ni magnetic moment in the h-BN/Ni(111) interface compared to bare Ni(111). This is backed by distortions of d-band features in the Fermi surface which indicate as well a decrease of the minority d-holes. Surface umklapps and reflections in the Fermi surface maps of h-BN/Ni(111) show that the h-BN layer acts as an efficient grating for electrons that scatter on this interface.

Acknowledgments

We thank R. Monnier for fruitful discussions. Funding from the Schweizerischen Nationalfonds is gratefully acknowledged.

References

1. M. Donath, *Surf. Sci. Rep.* **20**, 251 (1994).
2. M. N. Baibich, J. M. Broto, A. Fert, F. Nguyen Van Dau, F. Petroff, P. Etienne, G. Creuzet, A. Friedrich and J. Chazelas, *Phys. Rev. Lett.* **61**, 2472 (1988).
3. J. Maria De Teresa, A. Barthelemy, A. Fert, J. P. Contour, F. Montaigne and P. Seneor, *Science* **286**, 507 (1999).
4. A. Nagashima, N. Tejima, Y. Gamou, T. Kawai and C. Oshima, *Phys. Rev.* **B51**, 4606 (1995).
5. P. Blaha, K. Schwarz and J. Luitz, WIEN97, TU Vienna, 1997, updated UNIX version of the WIEN code as published by P. Blaha, K. Schwarz, P. Sorantin and S. B. Tickey, in *Comput. Phys. Commun.* **59**, 399 (1990).
6. T. Greber, W. Auwärter and J. Osterwalder, in *The Physics of Low Dimensional Systems*, ed.

J. L. Morán-López (Plenum, New York, 2001), pp. 411–418.
7. T. Greber, O. Raetzo, T. J. Kreutz, P. Schwaller, W. Deichmann, E. Wetli and J. Osterwalder, *Rev. Sci. Instrum.* **68**, 4549 (1997).
8. The value of 3.3 and 5.1 eV for the work function of h-BN/Ni(111) and Ni(111) quoted in an earlier publication[6] has to be corrected due to a 1% miscalibration of the energy scale of ΔE.
9. W. Auwärter, T. J. Kreutz, T. Greber and J. Osterwalder, *Surf. Sci.* **429**, 229 (1999).
10. Y. Gamou, M. Terai, A. Nagashima and C. Oshima, *Sci. Rep. RITU* **A44**, 211 (1997).
11. M. Muntwiler, W. Auwärter, F. Baumberger, M. Hoesch, T. Greber and J. Osterwalder, *Surf. Sci.* **472**, 125 (2001).
12. P. Aebi, J. Osterwalder, R. Fasel, D. Naumović and L. Schlapbach, *Surf. Sci.* **307–309**, 917 (1993).
13. J. Osterwalder, *Surf. Rev. Lett.* **4**, 391 (1997).
14. W. Eberhardt and E. W. Plummer, *Phys. Rev.* **B21**, 3245 (1980).
15. D. C. Tsui, *Phys. Rev.* **164**, 669 (1967).
16. R. F. W. Bader, *Atoms in Molecules: A Quantum Theory* (Oxford University Press, Oxford, 1990).
17. The "atom volume" is defined by a zero-flux surface, i.e. where for all points $\mathbf{r}_s$ on this surface the scalar product of the charge density gradient with the zero-flux surface normal $\mathbf{n}(\mathbf{r}_s)$ vanishes: $\nabla\rho(\mathbf{r}_s)\mathbf{n}(\mathbf{r}_s) = 0$.
18. G. Grad *et al.*, unpublished.
19. T. J. Kreutz, T. Greber, P. Aebi and J. Osterwalder, *Phys. Rev.* **B58**, 1300 (1998).
20. Elastic scattering cross sections were obtained from the optical theorem $[\sigma_{\mathrm{el}} = 4\pi\Im f(\vartheta = 0)/k]$. The imaginary part of the forward scattering amplitude was calculated from the scattering of a plane wave on the corresponding atomic potential. The phase shifts are determined with Pendry's MUFPOT program.
21. A. Adnot and J. D. Carette, *Phys. Rev. Lett.* **38**, 1084 (1977).
22. M. Lindroos, H. Pfnür, P. Feulner and D. Menzel, *Surf. Sci.* **180**, 237 (1987).